# Carbon-cluster formation from polymers caused by MeV-ion impacts and keV-cluster-ion impacts

C. W. Diehnelt, M. J. Van Stipdonk, and E. A. Schweikert*
*Center for Chemical Characterization and Analysis, Department of Chemistry, Texas A&M University, College Station, Texas 77843-3144*
(Received 16 November 1998)

It has been observed that under MeV-ion bombardment of a polymer, such as polycarbonate (PC) or polyvinylidene fluoride (PVDF), large quantities of carbon clusters ($C_n^-$ and $C_nH^-$) are generated. However, when PC or PVDF is bombarded with keV atomic ions, very few carbon-cluster ions are produced. This different behavior was attributed to the different sputtering/desorption mechanisms for keV- and MeV-ion impacts. Low-energy keV ions deposit their energy into a solid through nuclear stopping, while MeV ions deposit their energy mainly through electronic stopping. The formation of carbon clusters is thought to be facilitated by the high-temperatures and high-energy densities produced in the region nearest the point of MeV-ion impact, the infratrack region. We have observed extensive carbon-cluster formation from PC and PVDF under keV-cluster-ion bombardment. Despite the vastly different velocities of the high- and low-energy projectiles, identical carbon-cluster trends are produced from MeV $^{252}$Cf fission fragments and 20-keV $C_{60}^+$ projectile impacts on the same target. This leads us to the conclusion that a polyatomic ion impact, which deposits its kinetic energy near the surface, may create a region of high-temperature and high-energy density that is similar to the infratrack of a MeV-ion impact. [S1050-2947(99)00706-4]

PACS number(s): 34.50.Dy, 36.40.−c, 61.82.−d, 07.75.+h

## I. INTRODUCTION

The elucidation of the structure [1] of $C_{60}^+$ caused increased interest in carbon-cluster formation from various carbonaceous targets using several different techniques. For instance, laser vaporization, plasma desorption mass spectrometry (PDMS), and dynamic secondary-ion mass spectrometry (SIMS) have been used to generate carbon clusters from carbon targets. Feld and co-workers [2] compared the carbon-cluster production by MeV and keV atomic ion bombardment of several polymer substrates. They found that carbon clusters of the form $C_n^-$ and $C_nH^-$ were produced up to $n=21$ when $^{252}$Cf fission fragments impacted polycarbonate (PC). However, when PC was bombarded by $Ne^+$, $Ar^+$, or $Xe^+$ at 10–30 keV, carbon clusters were produced only up to $n=4$. Similar behavior was observed when polyvinylidene fluoride (PVDF) was used as the sample target. However, a surprising observation was that under MeV-ion bombardment, PVDF produced a carbon-cluster series out to $n=100$ with an enhanced abundance of $n=60$.

Recently, due to the high secondary-ion yields produced, there has been renewed interest in the use of polyatomic primary ions in SIMS. While the enhanced secondary-ion (SI) yield due to a polyatomic cluster impact is well known [3–17], there is much that is still unknown about the desorption mechanism for a keV energy cluster impact. It is widely known that the SI yield increases nonlinearly with the number of atoms in the cluster projectile. It is commonly believed that the enhanced yields are caused by regions of high collision density. It has been proposed that the nearly simultaneous impact of several atoms from a polyatomic projectile creates a region where numerous collision cascades overlap in both time and space [13]. This creates a local high collision density region where large amounts of material are sputtered. Whether the nonlinearity arises from increased sputter yields or increased ionization efficiency of the sputtered material has not been determined.

We have shown that large numbers of carbon-cluster anions are produced when small organic molecules are bombarded by keV polyatomic clusters [18]. In light of these findings and the earlier observations by Feld and co-workers [2], a study was undertaken with the intent to compare the behavior of keV cluster projectiles with MeV fission fragments. In this paper we present measurements of carbon-cluster emission caused by bombardment of PVDF and PC with $^{252}$Cf fission fragments (60–100 MeV), 20-keV monatomic primary ions, and 20-keV cluster ions.

## II. EXPERIMENTAL METHOD

The experiments were performed on a dual time-of-flight (TOF) mass spectrometer built in house, which has been described in detail elsewhere [17]. The vacuum of the system was maintained at $\sim 6.7\times10^{-5}$ Pa. One of a pair of fission fragments coemitted from a radioactive $^{252}$Cf source was used to produce atomic and cluster primary ions from a Mylar foil that was coated with CsI, ammonium hexafluorosilicate, indium (III) acetate, or $C_{60}$. The $In^+$ and $SiF_5^-$ foils were prepared by solution deposition while CsI and $C_{60}$ foils were prepared by vapor deposition. The second of the coemitted fission fragments impacted a detector, located 180°

*Author to whom correspondence should be addressed.
FAX: (409) 845-1655.
Electronic address: schweikert@mail.chem.tamu.edu

 

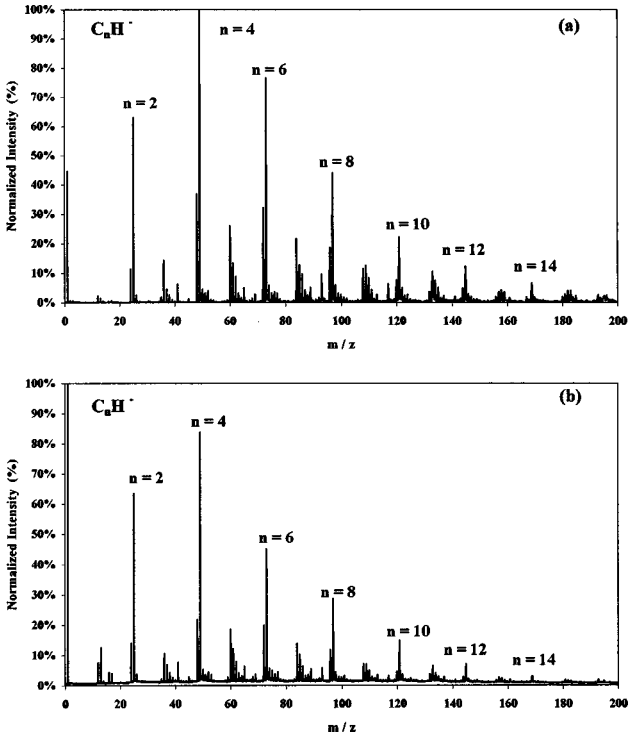


FIG. 1. Secondary-ion mass spectrum of PC produced by (a) fission fragment bombardment and (b) 20-keV $C_{60}^+$ bombardment. Each mass spectrum was divided by the relative yield of the most intense peak of that spectrum to provide the normalized intensity (%).

from the Mylar foil, which produced the start signal for the primary-ion TOF measurement. The cluster ions were accelerated to 20 keV and mass separated in the first TOF region. The primary ions struck a thick target of PVDF or PC on stainless steel with an incident angle of $\sim 27°$ with respect to the surface normal. The targets were prepared by dissolving $\sim 1$ mg of PVDF in acetone and $\sim 1$ mg of PC in cyclohexanone. The solutions were then deposited on the stainless steel sample support and allowed to dry.

To operate in PDMS mode, the Mylar source foil was removed, allowing fission fragments to traverse the flight tube and strike the target. When a primary ion strikes the surface, electrons are emitted and are used to register the arrival time of a particular projectile. Sputtered secondary ions are then mass analyzed in the second TOF region with a mass resolution $(m/\Delta m)$ greater than 300. The experiments were carried out in the event-by-event bombardment mode at the limit of single ion impacts. Typical primary ion doses were on the order of $10^5-10^7$ ions/cm$^2$, well within the static SIMS limit ($>10^{12}$ ions/cm$^2$). A coincidence counting data collection approach, developed in our laboratory [13], was used to obtain the ion yields produced from each primary-ion impact. Thus, the transmission and detection efficiencies of the instrument as well as the target surface conditions remained constant, allowing for direct comparison of the data from all cluster impacts. The relative yield (%) of each SI was calculated by integrating the area of the SI peak and dividing this number by the integrated area of the secondary electron peak, indicating the number of primary ions that impacted the surface.

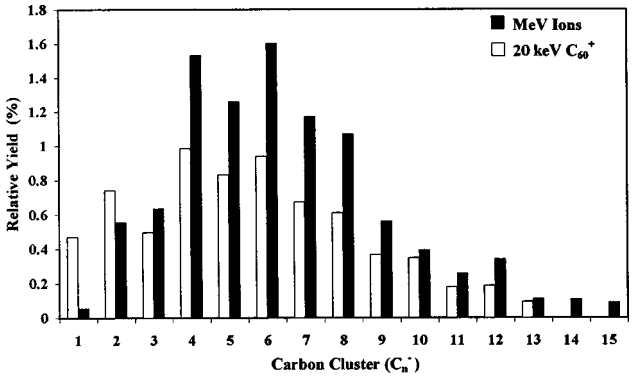


FIG. 2. Relative yield of $C_n^-$ $(n=1,2,\ldots)$ clusters from PC produced by MeV ions and 20-keV $C_{60}^+$.

## III. RESULTS

Figure 1(a) shows the SI mass spectrum generated by fission fragment impacts on PC. The spectrum is plotted such that all peak intensities are normalized to $C_4H^-$, the most intense peak in the spectrum. For the low-mass region, mass/charge $(m/z)<200$ amu, a large carbon-cluster distribution is observed. $C_nH^-$ clusters were observed up to $n=16$, however, no clusters after $n=16$ could be determined above the background spectrum. Note the strong even-odd cluster distribution which is thought to arise from the high electron affinity of the even carbon clusters [19].

The same PC sample was bombarded with 20-keV $C_{60}^+$ primary ions. The resulting mass spectrum is shown in Fig. 1(b). The carbon-cluster distribution observed is qualitatively the same as that seen using PDMS. Once again, the background signal obscured any carbon clusters formed past $n=16$. The spectra produced by $(CsI)Cs^+$ and $SiF_5^-$ cluster bombardment (spectra not shown) exhibit a similar but less extensive series of carbon clusters. In the spectrum of PC produced by $SiF_5^-$, a peak at $m/z$ 19 was observed, which was absent using all other projectiles. This is in line with our earlier observation of F recoiling from fluorinated cluster projectiles upon impact with an organic target [20].

The relative yield of each bare carbon cluster, $C_n^-$, emitted from PC is plotted in Fig. 2 for fission fragment and $C_{60}^+$ bombardment. The trends are almost identical except for a switch of intensities for $n=1$ and 2. Since these two carbon-cluster peaks arise primarily from hydrocarbon contaminants

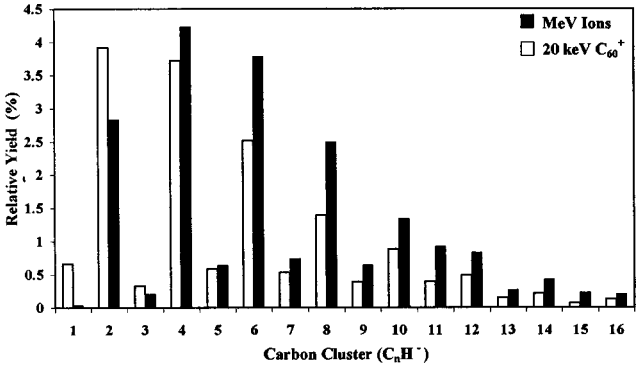


FIG. 3. Relative yield of $C_nH^-$ $(n=1,2,\ldots)$ clusters from PC generated by MeV ions and 20-keV $C_{60}^+$.

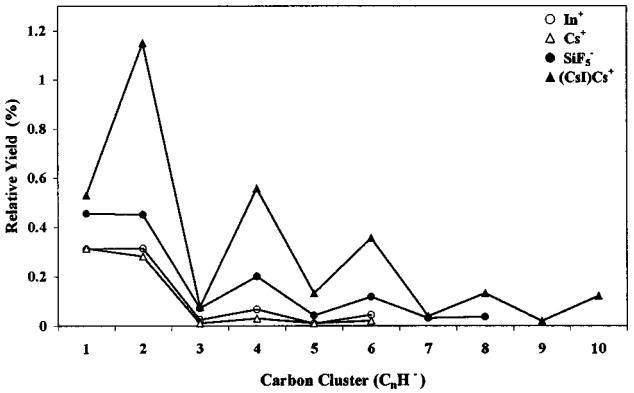


FIG. 4. Relative yield of $C_nH^-$ ($n=1,2,\ldots$) clusters from PC produced by 20-keV $In^+$, $Cs^+$, $SiF_5^-$, and $(CsI)Cs^+$ projectiles.

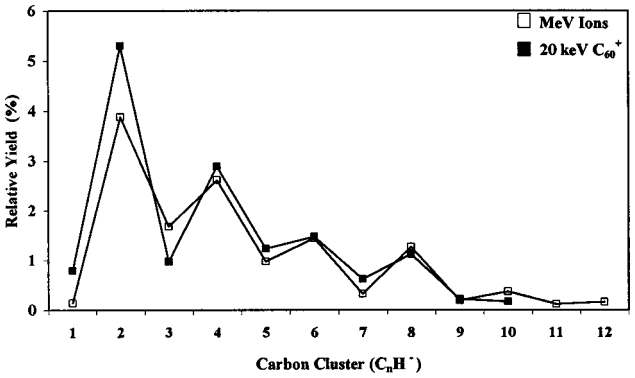


FIG. 6. Relative yield of $C_nH^-$ ($n=1,2,\ldots$) clusters from PVDF generated by MeV ions and 20-keV $C_{60}^+$.

on the surface [18], the aberration is expected due to the increased surface sensitivity of $C_{60}^+$ caused by its shallow penetration depth.

In Figs. 3 and 4, the relative yield of each $C_nH^-$ cluster is plotted for all projectiles. The graph in Fig. 3 shows that the $C_nH^-$ cluster trend produced by MeV ions and 20-keV $C_{60}^+$ is the same. The cluster yield from $(CsI)Cs^+$ and $SiF_5^-$, as well as the atomic primary ions, $In^+$ and $Cs^+$, is shown in Fig. 4. The carbon-cluster formation from the atomic primary ions ceases at $n=6$, in accord with the results of Feld and co-workers [2]. When $(CsI)Cs^+$ or $SiF_5^-$ are used, $C_nH^-$ clusters are produced out to $n=10$ and 8, respectively. This result is further discussed below.

A sample of PVDF was analyzed with our series of projectiles (spectra not shown). The low-mass carbon-cluster formation was less extensive than from PC. Higher-mass carbon clusters, such as $C_{60}^-$, were not observed. The relative yields of $C_n^-$ clusters for PDMS and $C_{60}^+$ are shown in Fig. 5. The $C_{60}^+$ trend mirrors the PDMS trend with the expected deviations for the low-mass contaminant clusters. The higher intensity of the $n=10$ peak for $C_{60}^+$ is within the error of our experiment and not considered significant.

Figures 6 and 7 show the $C_nH^-$ cluster yields from fission fragment impacts and from each cluster projectile. The PDMS and $C_{60}^+$ series are very similar. Although $C_{60}^+$ led to higher abundances of the $n=4$, 5, 6, and 7 clusters, within the error of our measurements, the differences are not significant. The same trends hold for $(CsI)Cs^+$ and $SiF_5^-$, with one notable difference. For PVDF, $(CsI)Cs^+$ and $SiF_5^-$ form the same number of $C_nH^-$ clusters. This could be due to chemical effects which will be described in detail later.

## IV. DISCUSSION

A mechanism for the production of carbon clusters from PVDF was proposed [2] whereby the polymer undergoes carbonization and subsequent degradation to form large carbon clusters. Upon ion impact, the polymer undergoes dehydrohalogenation at one chain side of the polymer. The products of this reaction are a conjugated polyene and HF. The polyene then loses all substituents to form bare carbon and HF.

Within the framework of this mechanism, Feld and coworkers resolved the differences between SIMS, where no $C_{60}$ was formed, and PDMS. In SIMS, the primary ion deposits its energy through nuclear collisions, leading to a large yield of products from the first reaction step. Due to the electronic excitation induced by a MeV fission fragment, the second step of the degradation reaction is favored and for PDMS, products of the second step dominate.

Following this work, Sundqvist and co-workers at Uppsala performed numerous studies of the formation of low-mass and high-mass carbon clusters from several polymers under MeV-ion bombardment [21–27]. All experiments

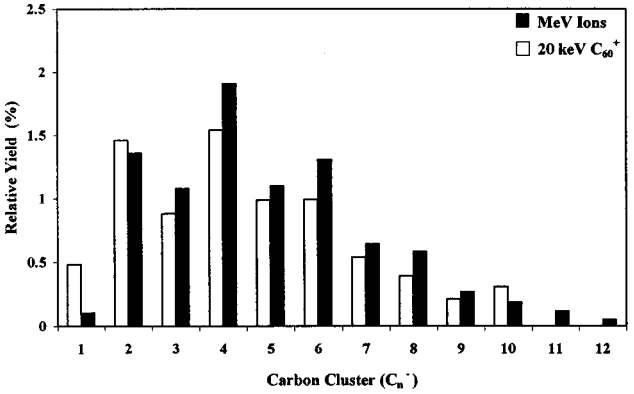


FIG. 5. Relative yield of $C_n^-$ ($n=1,2,\ldots$) clusters from PVDF produced by MeV ions and 20-keV $C_{60}^+$.

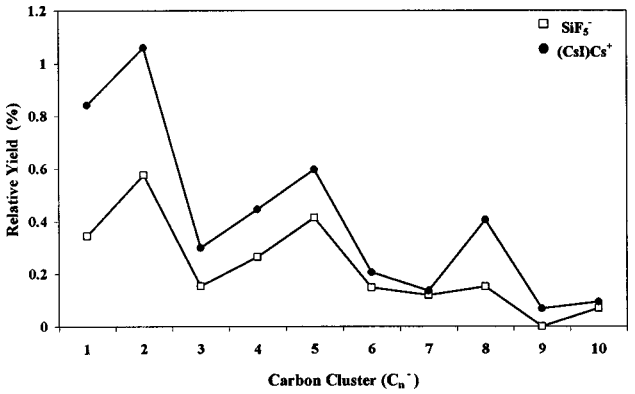


FIG. 7. Relative yield of $C_nH^-$ ($n=1,2,\ldots$) clusters from PVDF produced by 20-keV $SiF_5^-$ and $(CsI)Cs^+$ projectiles.

were performed using a low primary-ion current, ensuring that each incident particle impacted an undamaged area of the polymer. Their work showed that carbon clusters were formed by a single MeV-ion impact and not by a collective effect due to the primary beam dose. By studying the radial velocities of emitted clusters, Fenyö and co-workers [24] were able to determine that low-mass ions such as $CH_3^+$ and $C_2H_3^+$ were thermally evaporated. This finding led Papaléo and co-workers [25] to examine the radial velocities of positively charged $C_nH_m$ ions emitted from PVDF and polystyrene (PS). They found that the radial velocities of the carbon clusters changed with increasing hydrogenation. Pure carbon clusters, $C_n^+$, were found to be emitted from the high-temperature infratrack region closest to the MeV-ion impact site, while carbon clusters with a higher hydrogen content were emitted from a lower energy density region removed from the hot infratrack core.

When negatively charged $C_nH_m$ clusters were examined [25], the radial velocity distributions from PVDF and PS targets showed no dependence on the hydrogen content of the cluster. Two hypotheses were suggested to account for this behavior. These ions could be ejected after the infratrack has neutralized and cooled, or negative carbon clusters could be formed outside the positively charged infratrack. However, both of these explanations are speculative and no definitive conclusion about the origin of negative carbon clusters was reached.

By coupling these data with disappearance cross sections $\sigma_i$, measured from PVDF, Papaléo and co-workers [26] were able to develop a picture of the energy density and structure of a MeV-ion track. The disappearance cross section is determined by monitoring the decrease in intensity of a particular secondary ion as a function of primary-ion dose. It was found that the disappearance cross section, equivalent to the ejection radius of a specific ion, increases with increasing hydrogenation of the carbon cluster. This finding confirmed the radial velocity data which showed that ions with fewer hydrogen atoms originated from the hotter areas of the ion track. In this way, the emission of positive clusters was directly correlated to the energy density of different regions of the MeV-ion track.

An important effect in a polyatomic cluster impact is the overlap between multiple collision cascades in both time and space. In a cluster projectile, the total kinetic energy is partitioned between the constituent atoms of the projectile. This lowers the energy per incident atom, which decreases the penetration and range of each projectile atom. The decreased penetration depth allows the energy deposited by a cluster to be concentrated in the surface to near-surface region, creating a region of high-energy density. For example, a transport of ions in matter (TRIM) calculation [28] of a 333-eV C atom impact on PC yields a penetration depth of $\sim$2.5 nm. While a single $C_{60}^+$ projectile might penetrate to a depth greater than 2.5 nm due to a ''clearing the way effect'' [29], the penetration depth is still less than the 22.4-nm range of a 20-keV Cs atom and several orders of magnitude less than a MeV ion. Each 333-eV C atom from 20-keV $C_{60}^+$ will initiate a collision cascade near the surface, leading to a region of very high collision density. The effects of this collisionally excited region could be manifested as a local region of high pressure and high temperature due to the numerous collisions between atoms. Within this context, it is probable that a 20-keV $C_{60}^+$ projectile, with 60 simultaneous collision cascades occurring within 2.5 nm of the surface, could create a high-temperature, high-energy density region very similar to the high-temperature, high-energy density infratrack of a MeV-ion impact. This would explain the similar carbon cluster trends produced by MeV fission fragments and 20-keV $C_{60}^+$.

Within this qualitative model, the formation of carbon clusters can be used as a qualitative indication of the energy density of each primary ion. $(CsI)Cs^+$, which has a lower-energy density than $C_{60}^+$ due to the increased penetration depth and fewer collision cascades, would produce a smaller region of the high-energy density needed to produce small carbon clusters. Hence, $(CsI)Cs^+$ produces fewer carbon clusters than do $C_{60}^+$ or MeV ions from both PC and PVDF. $SiF_5^-$ has a lower-energy density than $(CsI)Cs^+$ because the impact of a Cs or I atom will lead to a larger collision cascade than the impact of a single Si or F atom. This is the well-known mass effect of the primary ion in SIMS. Consequently, the lower-energy density of $SiF_5^-$ relative to $(CsI)Cs^+$ manifests itself by producing fewer carbon clusters than $(CsI)Cs^+$ for the case of PC. The case of $SiF_5^-$ having an identical carbon-cluster trend with $(CsI)Cs^+$ for PVDF is a special case which will be discussed below.

It has been reported [2] that PVDF produces $C_{60}^+$ secondary ions whereas other polymers, such as Teflon, do not do so under MeV-ion bombardment. The conclusion was that hydrogen and fluorine, present in PVDF, rapidly form HF which is necessary for large even number carbon-cluster formation. If this mechanism holds true, this could explain the similarity between $(CsI)Cs^+$ and $SiF_5^-$ carbon-cluster yields from PVDF. We have observed [20] the ejection of constituents of a polyatomic cluster projectile, namely, F ions from $(NaF)_nNa^+$, $BF_4^-$, $PF_6^-$, and $SiF_5^-$ upon impact. The presence of F at the impact site could facilitate carbon-cluster formation by abstracting hydrogen from PVDF to form HF.

## V. CONCLUSIONS

We have shown that the polymers PC and PVDF emit large numbers of negative carbon clusters under bombardment by MeV ions and 20-keV polyatomic ions. The yield trend of carbon-cluster ions is virtually identical between PDMS and 20-keV $C_{60}^+$. The other polyatomic projectiles examined, $(CsI)Cs^+$ and $SiF_5^-$, produce more carbon clusters than 20-keV monatomic primary ions, $Cs^+$ and $In^+$, but fewer than $C_{60}^+$ or fission fragments. It has been reported that positive carbon clusters are formed in the hot high-energy density region of the infratrack of a MeV-ion impact [21–27]. If negative carbon clusters are formed in similar high-temperature regions of the ion track, then the similar behavior of $C_{60}^+$ and PDMS can be attributed to each projectile producing a region of high-temperature and high-energy density that facilitates carbon-cluster formation.

## ACKNOWLEDGMENT

This work was supported by the National Science Foundation (Grant No. CHE-9727474).

[1] H. W. Kroto, J. R. Heath, S. C. O'Brien, R. F. Curl, and R. E. Smalley, Nature (London) **318**, 162 (1985).
[2] H. Feld, R. Zurmühlen, A. Leute, and A. Benninghoven, J. Phys. Chem. **94**, 4595 (1990).
[3] A. D. Appelhans and J. E. Delmore, Anal. Chem. **59**, 1685 (1987).
[4] J. F. Mahoney, J. Perel, T. D. Lee, and J. Legesse, Int. J. Mass Spectrom. Ion Processes **79**, 249 (1987).
[5] A. D. Appelhans and J. E. Delmore, Anal. Chem. **61**, 1087 (1989).
[6] M. G. Blain, S. Della-Negra, H. Joret, Y. Le Beyec, and E. A. Schweikert, Phys. Rev. Lett. **63**, 1625 (1989).
[7] M. G. Blain, S. Della-Negra, H. Joret, Y. Le Beyec, and E. A. Schweikert, J. Phys. (Paris), Colloq. **50**, C2-147 (1989).
[8] J. E. Delmore, A. D. Appelhans, and D. A. Dahl, Rev. Sci. Instrum. **61**, 633 (1990).
[9] E. A. Schweikert, M. G. Blain, M. A. Park, and E. F. da Silveira, Nucl. Instrum. Methods Phys. Res. B **50**, 307 (1990).
[10] J. F. Mahoney, J. Perel, S. A. Ruatta, P. A. Martino, S. Husain, and T. D. Lee, Rapid Commun. Mass Spectrom. **5**, 441 (1991).
[11] M. A. Park, E. A. Schweikert, E. F. da Silveira, C. V. Barros Leite, and J. M. F. Jeronymo, Nucl. Instrum. Methods Phys. Res. B **56/57**, 361 (1991).
[12] M. Benguerba, A. Brunelle, S. Della-Negra, J. Depauw, H. Joret, Y. Le Beyec, M. G. Blain, E. A. Schweikert, G. Ben Assayag, and P. Sudraud, Nucl. Instrum. Methods Phys. Res. B **62**, 8 (1991).
[13] M. A. Park, B. D. Cox, and E. A. Schweikert, J. Chem. Phys. **96**, 8171 (1992).
[14] P. A. Demirev, J. Eriksson, R. A. Zubarev, R. Papaléo, G. Brinkmalm, P. Håkansson, and B. U. R. Sundqvist, Nucl. Instrum. Methods Phys. Res. B **88**, 139 (1994).
[15] W. Szymczak and K. Wittmaack, Nucl. Instrum. Methods Phys. Res. B **88**, 149 (1994).
[16] K. Boussofiane-Baudin, G. Bolbach, A. Brunelle, S. Della-Negra, P. Håkansson, and Y. Le Beyec, Nucl. Instrum. Methods Phys. Res. B **88**, 160 (1994).
[17] M. J. Van Stipdonk, R. D. Harris, and E. A. Schweikert, Rapid Commun. Mass Spectrom. **10**, 1987 (1996).
[18] C. W. Diehnelt, M. J. Van Stipdonk, and E. A. Schweikert, in *Secondary Ion Mass Spectrometry: SIMS XI*, edited by G. Gillen, R. Lareau, J. Bennett, and F. Stevie (Wiley, Chichester, 1998), p. 593.
[19] M. LeLeyter and P. Joyes, Radiat. Eff. **18**, 105 (1973).
[20] C. W. Diehnelt, M. J. Van Stipdonk, and E. A. Schweikert, Nucl. Instrum. Methods Phys. Res. B **142**, 606 (1998).
[21] G. Brinkmalm, D. Barofsky, P. Demirev, D. Fenyö, P. Håkansson, R. E. Johnson, C. T. Riemann, and B. U. R. Sundqvist, Chem. Phys. Lett. **191**, 345 (1992).
[22] R. M. Papaléo, A. Hallén, P. Demirev, G. Brinkmalm, J. Eriksson, P. Håkansson, and B. U. R. Sundqvist, Nucl. Instrum. Methods Phys. Res. B **91**, 677 (1994).
[23] G. Brinkmalm, P. Demirev, D. Fenyö, P. Håkansson, J. Kopniczky, and B. U. R. Sundqvist, Phys. Rev. B **47**, 7560 (1993).
[24] D. Fenyö, A. Hedin, P. Håkansson, and B. U. R. Sundqvist, Int. J. Mass Spectrom. Ion Processes **100**, 63 (1990).
[25] R. M. Papaléo, G. Brinkmalm, D. Fenyö, J. Eriksson, H.-F. Kammer, P. Demirev, P. Håkansson, and B. U. R. Sundqvist, Nucl. Instrum. Methods Phys. Res. B **91**, 667 (1994).
[26] R. M. Papaléo, P. A. Demirev, J. Eriksson, P. Håkansson, and B. U. R. Sundqvist, Int. J. Mass Spectrom. Ion Processes **152**, 193 (1996).
[27] R. M. Papaléo, P. Demirev, J. Eriksson, P. Håkansson, B. U. R. Sundqvist, and R. E. Johnson, Phys. Rev. Lett. **77**, 667 (1996).
[28] J. F. Ziegler, J. P. Biersack, and U. Littmark, in *The Stopping and Ranges of Ions in Solids*, edited by J. F. Ziegler (Pergamon, New York, 1985), Vol. 1.
[29] V. I. Shulga and P. Sigmund, Nucl. Instrum. Methods Phys. Res. B **62**, 23 (1991).